Rheologica Acta Rheol Acta 23:20–30 (1984)

Shear flow rheological properties of vinylon- and glass-fiber reinforced polyethylene melts

T. Kitano, T. Kataoka, and Y. Nagatsuka

Research Institute for Polymers and Textiles, Ibaraki (Japan)

Abstract: Shear viscosity, shear stress and first normal-stress difference have been investigated for glass- and vinylon-fiber filled polyethylene melts over a wide range of shear rate by means of three kinds of instruments. The influence of fiber content and fiber properties on the rheological properties is discussed. The viscosity increases with increasing aspect ratio and fiber content, and the influence of these parameters on the flow properties is evident at low shear rates. The first normal-stress difference increases more rapidly with increasing glass fiber content, especially at low shear stresses. The influence of vinylon fibers on the first normal stress-difference vs. shear-stress relationship is different from that of glass fibers.

Key words: Viscosity, first normal-stress difference, fiber filled polymer melt, glass fiber, vinylon fiber

1. Introduction

According to the growing use of fiber reinforced thermoplastics several papers [1–3] have reported on the rheological properties of polymer melts filled with fibers, but these deal solely with glass-fiber filled melts and are limited to high shear flow viscosity measurements. Still recently a few studies of the shear-flow viscosity and the first normal-stress difference of fiber filled polymer melts in the low shear rate region did appear [4–7].

In our previous papers [8–10] we studied the flow properties of polymer melts filled with glass-fibers, carbon-fibers and a few kinds of particles, and discussed the effect of length, length distribution, aspect ratio and fiber damage in mixing process etc. on the flow characteristics of melts. There was little consideration on the influence of fiber type and properties (i.e. rigid or flexible fibers or deformable fibers induced by shear flow) with the exception of a few studies [7–11].

In this paper, we consider the effect of the difference in characteristics of glass-fibers and vinylon-fibers on the rheological properties of polymer melts filled with these fibers over a wide range of shear rates.

2. Experimental

2.1 Materials

The systems investigated in this study were polyethylene melts filled with glass and vinylon fibers. Polyethylene (PE) was "Flowthene" G701 manufactured by Seitetsu Kagaku Ind. Co. Ltd., and had MFR (190 °C, 2.16 kg) of 7.8. Glass fibers from Nitto Boseki Co. Ltd. (GF, CSX6PE, 3 denier, 6 mm, 200 filaments) and four kinds of vinylon fibers from Kuraray Co. Ltd. (VF6, 6 denier, 1, 3, 5 mm and VF1, 1 denier, 1 mm) were used as fillers. The characteristics and codes of these fibers are summarized in table 1.

Weighted amounts of PE and fibers (chopped strands) were supplied to a 25 mm ∅ extruder which operated at 180 °C with a screw rotation of 40 rpm. After extrudate was passed in a water bath, it was cut into tips of about 5 mm length by a pelletizer. After drying in an air oven, tips were collected and mixed thoroughly. The mixture was again extruded. This operation was repeated two times by a Fullflight type screw. The dispersion of fibers (coloured vinylon fibers were used) examined by a photomicrograph was rather

Table 1. Fiber Characteristics

Characteristics	Glass Fiber (GF)	Vinylon Fiber (VF)
Density (g/cm^3)	2.52	1.26
Diameter (μm)	13.6	11.3, 26.8
Tensile moduli (kg/mm^2) (25 °C)	6500	1200
Tensile strength (kg/mm^2) (25 °C)	100	80
Critical strain (%) (25 °C)	1.86	14.3

Table 2. Sample codes and content of fibers

Code	Weight fraction Φ_w(%)	Volume fraction Φ(%)	Fiber
GF-20	20	8.4	$l = 0.26-0.42$ mm
GF-30	30	13.5	$d = 13.6$ μm
GF-40	40	19.6	aspect ratio
GF-50	50	26.8	$a_r = l/d = 20-30$
VF61-3	3	2.2	$l = 1.22$ mm
VF61-5	5	3.7	$d = 26.8$ μm
VF61-10	10	7.5	$a_r = 45$
VF61-15	15	11.4	
VF63-3	3	2.2	$l = 3.23$ mm
VF63-5	5	3.7	$d = 26.8$ μm
FV63-10	10	7.5	$a_r = 120$
VF65-3	3	2.2	$l = 5.02$ mm
VF65-5	5	3.7	$d = 26.8$ μm
VF65-10	10	7.5	$a_r = 180$
VF11-3	3	2.2	$l = 1.28$ mm
VF11-5	5	3.7	$d = 11.3$ μm
VF11-10	10	7.5	$a_r = 110$

well, independent of fiber size and content. In this paper, therefore, data were treated assuming that the dispersion of fibers is good enough to discuss the flow properties of these systems. Table 2 summarizes the sample codes, weight and volume fractions of fibers employed in this study at 180 °C.

2.2 *Rheological measurements*

Measurements of the steady-state shear stress $\sigma_{12}(\dot{\gamma})$ and the first normal-stress difference $N_1(\dot{\gamma})$ at relatively low shear rates $\dot{\gamma}$ ($5 \times 10^{-3} - 10\ s^{-1}$) were carried out with a cone-plate-type rheogoniometer (CPRM; cone radius $R = 2.15$ cm, cone gap $h = 200$ μm, and cone angle $\theta = 4°$; RGM 151-S, Nippon Rheology Kiki Co. Ltd.). The shear stress was measured through the torque T, and the first normal-stress difference through the thrust F, using the expressions [12]

$$\sigma_{12} = 3T/2\pi R^3, \quad N_1 = 2F/\pi R^2. \tag{1}$$

The shear rate in the gap is given by

$$\dot{\gamma} = \Omega/\theta \tag{2}$$

where Ω is the angular velocity. The flow properties of the fiber-filled melts in the intermediate shear rate region ($\dot{\gamma} = 10 - 50\ s^{-1}$) were measured by using a slit-type die attached to the extruder. The dimensions of the rectangular slit die was as follows: slit width $W = 40$ mm, thickness $h = 1$ mm, aspect ratio $W/h = 40$ and length $L = 130$ mm.

Four pressure tranducers (HPB 100N-350-EX, Toyo Boldwin Co. Ltd.) were flush-mounted on the long side of the rectangular slot along the longitudinal axis (z), and the pressure profiles along the axis were measured. The wall shear stress σ_w was determined by using the expression [13]

$$\sigma_w = (-\partial p/\partial z)\, h/2 \tag{3}$$

in which $-\partial p/\partial z$ is the slope of the pressure profile. Since the aspect ratio of the slit die is large enough, the flow can be considered as one-dimensional, and the apparent wall shear rate $\dot{\gamma}_w$ may be defined as

$$\dot{\gamma}_w = 6Q/W h^2 \tag{4}$$

where Q is the volumetric flow rate.

The true wall shear rate $\dot{\gamma}$ may be calculated by means of the Rabinowitch-Mooney correction as

$$\dot{\gamma} = \left(\frac{2n+1}{3n}\right)\dot{\gamma}_w \tag{5}$$

where n is defined by $n = d\ln\sigma_w/d\ln\dot{\gamma}_w$. Extrapolation of the pressure profile to the exit of the slit die enables us to find the value of the wall normal stress at the exit, which is referred to as "exit pressure". The exit pressure P_{exit} can be considered to be approximately equal to the normal-stress difference N_1 [13], i.e.

$$N_1 \approx P_{exit}. \tag{6}$$

The flow characteristics of fiber filled melts at high shear rates ($\dot{\gamma} = 10 - 10^5\ s^{-1}$) were measured by using a capillary viscometer (Koka-shiki Flow tester, Shimazu Seisakusho Co. Ltd.). Four kinds of capillary dies having the same radius ($r = 0.5$ mm) and different lengths ($l = 2$, 4, 6 and 10 mm) were employed. The correction factor, e, at a constant shear rate can be determined from plots of the pressure in a reservoir, P, against l/r, which are called Bagley plots. Wall shear

stress σ_w and true shear rate $\dot{\gamma}$ are given by

$$\sigma_w = \frac{P}{2(l/r + e)} \tag{7}$$

$$\dot{\gamma} = 4\,Q/\pi r^3 \left\{\frac{3}{4} + \frac{1}{4}\,\frac{d \ln 4\,Q/\pi r^3)}{d \ln \sigma_w}\right\} \tag{8}$$

where Q is the volumetric flow rate. All experiments were conducted at a controlled temperature of 180 °C.

3. Results and discussion

A few typical examples of the distributions of glass fiber lengths in the samples are shown in figure 1. The damage of glass fibers (GF) occurs rapidly in the mixing process with an extruder, and fracture surfaces of damaged GF are seen to be clean from the photomicrographs. The distribution of GF lengths changes and the number average length l_m defined as

$$l_m = \frac{\sum n_i l_i}{\sum n_i} = \frac{\sum n_i l_i}{N} \tag{9}$$

becomes smaller with increasing fiber content. The number N in these experiments was about 800.

The breakage and mastication in this mixing process are more rapid and severe for GF than for vinylon fibers (VF). VF may become shorter, although only slightly, in the process of cutting the extrudate by a pelletizer, and the distribution of lengths becomes although slightly wider. The contraction rate of VF is about 2% below 230 °C at a rate of 1 °C/minute in air [21]. Although the contraction rate of VF in polymer melts at 180 °C was not examined, we expected it to be smaller than 2% and neglected it in the calculation of the volume fraction in polymer melts. VF did not exhibit bending or kinking which were found for Kevler fibers in polymer melts [7]. Forgacs and Mason [13] undertook studies of particle motions and deformations of fibers having various moduli and diameters and presented an analysis for buckling of fibers, whereas Czarnecki and White [7] determined the relation between the bending stress σ_b and l/d (aspect ratio, a_r) for this to occur. A glass fiber can be broken by bending strengths, although its l/d is very small.

In figures 2–4, the viscosity and the shear stress measured by CPRM and a slit flow apparatus (SLIT) are plotted against the shear rate for GF-PE and VF-61-PE systems. The shear stress was calculated by eqs. (1) and (3), and the shear rate by eqs. (2) and (5), respectively. The viscosity η is given as the ratio of shear stress to shear rate. As is evident from the figures, the shear stress and the viscosity are increased by filling with fibers, and the latter decreases with increasing shear rate. Measurements by CPRM become difficult with increasing shear rate and fiber content. The slope of shear-stress curves at low shear rates for GF-PE systems is almost equal to unity (fig. 2), indicating that the viscosity is constant. Non-Newtonian behavior can be observed at shear rates higher than about $10^{-1}\,s^{-1}$, and the viscosity decreases rapidly with increasing shear rate. The flow curves obtained by two different types of apparatus are fairly smoothly connected at high shear rates.

Flow behavior of VF61-PE systems (fig. 3) is similar to that of GE-PE systems as a whole, but we can find some different phenomena for VF61-PE systems at low shear rates. Firstly, the rate of increase in the viscosity and shear stress with volume fraction of fibers, Φ, of VF61-PE systems in the lower shear rate region is larger than those of GF-PE systems. Secondly, non-Newtonian behavior appears in this region for VF61-PE systems. These results may be due to the difference in aspect ratios between VF and GF, and also to the difference in the structures composed by both fibers with different flexibilities. Shear stress and viscosity curves for both the systems change parallel with those of PE in the intermediate and high shear-

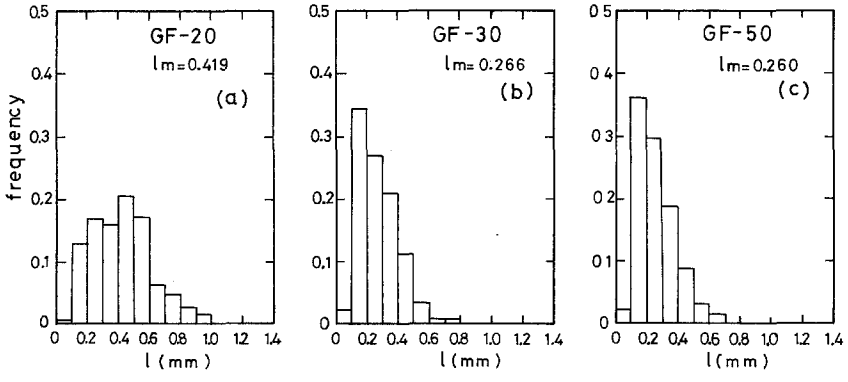

Fig. 1. Distribution of the fiber-lengths of GF-PE systems. (a) GF-20, (b) GF-30, (c) GF-50. The average length l_m and the average aspect ratio a_r are as follows:

	l_m (mm)	a_r
GF-20	0.419	30
GF-30	0.266	20
GF-50	0.260	19

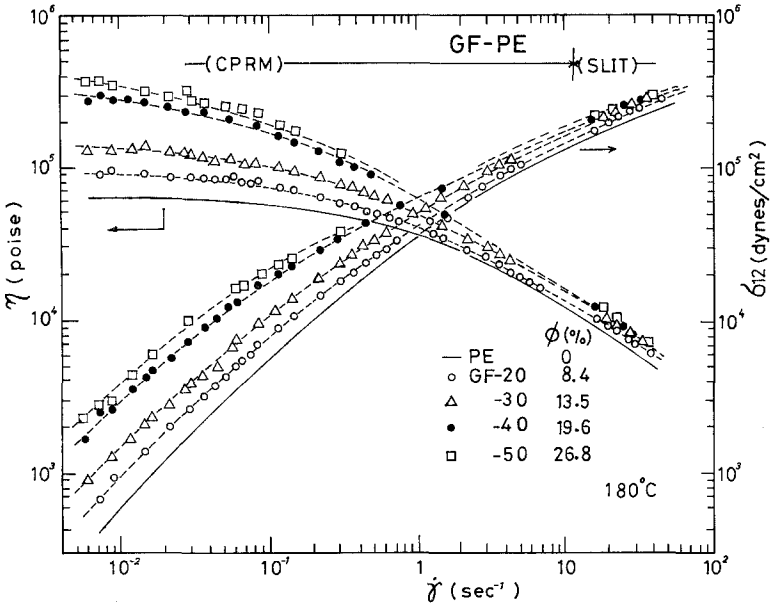

Fig. 2. Relation between shear stress σ_{12} and shear rate $\dot{\gamma}$, as well as viscosity η and shear rate $\dot{\gamma}$ of GF-PE systems at 180 °C.

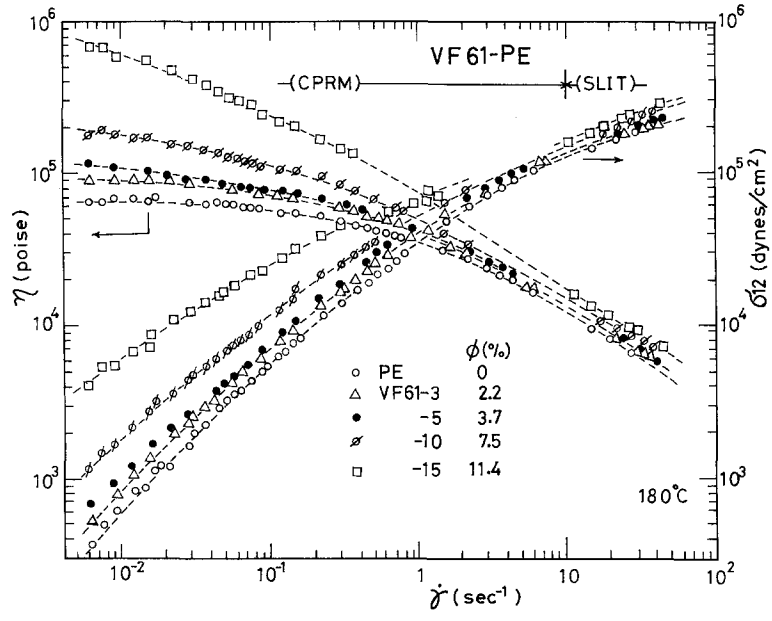

Fig. 3. Relation between shear stress σ_{12} and shear rate $\dot{\gamma}$, as well as viscosity η and shear rate $\dot{\gamma}$ of VF61-PE systems at 180 °C.

rate regions. Flow curves for various VF-PE systems are shown in figure 4, in which Φ was kept to be 3.7% and 7.5%, but lengths and diameters of fibers were different. Viscosity at the same Φ depends on the size (length and diameter) of VF.

The viscosity tends to increase with increasing aspect ratio of VF, but the viscosity of VE-PE systems is not high as compared with VF suspensions in silicone oil or polymer solutions [14–15]. Only for VF11-PE systems, the viscosity becomes lower than that of any other VF-PE system in the case of $\Phi = 7.5\%$. The non-Newtonian flow properties appear at low shear rates for $\Phi = 7.5\%$

Forces which tend to bend and buckle a rotating fiber act on the surface of a fiber in a shear flow field, and a flexible vinylon fiber which is not so rigid as a glass fiber will deform to the flow direction easier than a glass fiber. The difference in sizes and properties of the fibers is responsible for the difference in the flow properties of the systems examined in this study.

It seems convenient to introduce a concept of relative viscosity in order to interpret the influence of fillers on

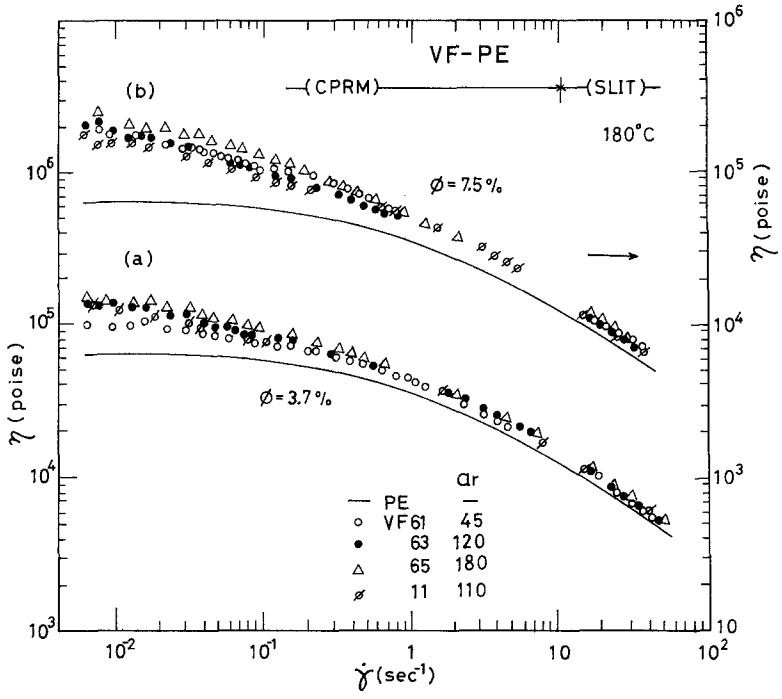

Fig. 4. Viscosity η as a function of shear rate $\dot{\gamma}$ for the PE melts filled with four kinds of VF. (a) $\Phi = 3.7\%$, (b) $\Phi = 7.5\%$.

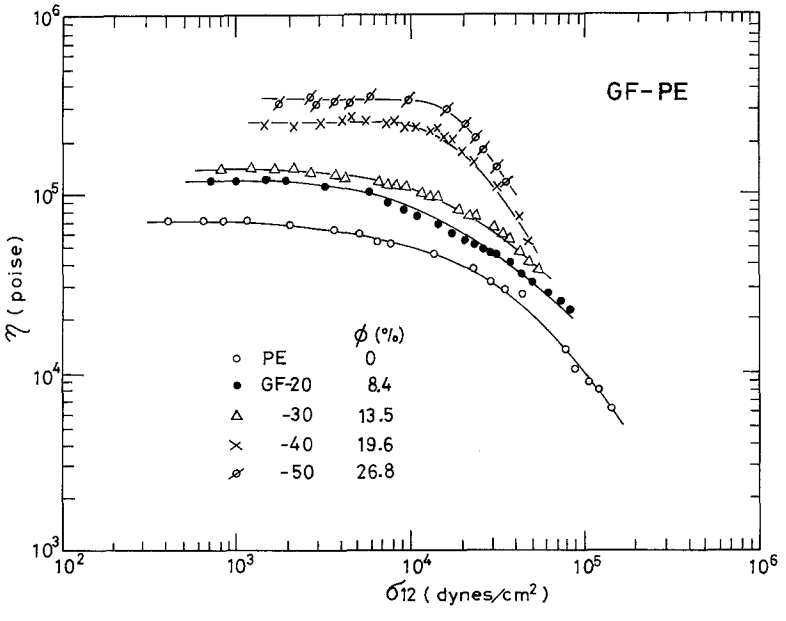

Fig. 5. Viscosity η as a function of shear stress Φ_{12} for GF-PE systems.

the viscosity of suspensions. There are two kinds of definitions of the relative viscosity η_r. The first is defined as the ratio of the viscosity of fiber-filled suspension to that of the medium at the same shear rate, and the second as the ratio of viscosities at the same shear stress. In preceding papers [9, 10] we obtained the following relations between fiber content Φ and the latter relative viscosity η_r:

$$\eta_r = (1 - \Phi/A)^{-2}, \tag{10}$$

$$A = a - b \cdot a_r \tag{11}$$

where a and b are experimental constants. These equations were derived on the basis of Maron-Pierce's

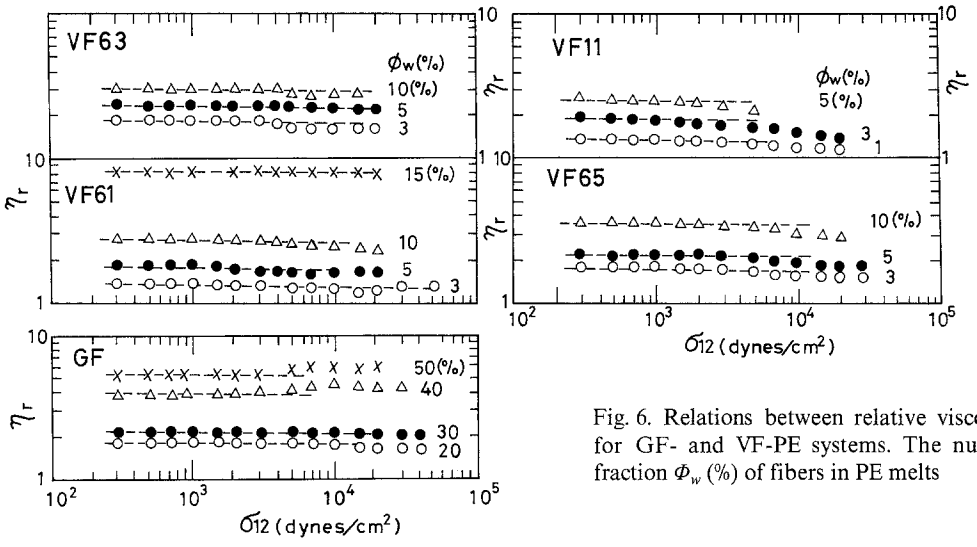

Fig. 6. Relations between relative viscosity η_r and shear stress σ_{12} for GF- and VF-PE systems. The numbers designate the weight fraction Φ_w (%) of fibers in PE melts

equation

$$\eta_r = (1 - \Phi/\Phi_0)^{-2}.$$

A in eq. (11) is a parameter relating to the packing geometry of the fillers and is considered to be similar to Φ_0 in Maron-Pierce's equation. As an example of the relation between η and σ_{12} figure 5 shows data obtained for GF-PE systems. Figure 6 shows the plots of η_r and σ_{12} for GF- and VF-PE systems with various fiber contents. It is seen from these figures that constant values of η_r can be obtained within the attainable shear stresses. From the above results the values of η_r can be estimated. η_r of suspensions at the same Φ varies with the properties of the filler such as shape, size, size-distribution, surface appearance etc. The value of η_r of each series increases, of course, with increasing Φ of the filler. Figure 7 shows semi-logarithmic plots of η_r against Φ of various systems. From the relation between η_r and Φ for various kinds of fibers having different aspect ratios smaller than about 40, we evaluated a and b of eq. (11) and obtained $a = 0.54$ and $b = 0.0125$ [10]. It was impossible to apply eq. (11) for VF-PE systems in which aspect ratios of VF are larger than than 100. Eq. (11) has to be corrected when it is applied to suspensions of fibers with large aspect ratios and flexibility. The numerical values in figure 7 represent values of A calculated using eq. (11) for GF-PE systems [10]. Finally, for VF-PE systems, eq. (10) was used by the best fitting method because eq. (11) could not be applied.

The first normal-stress difference N_1 as a function of the shear rate $\dot{\gamma}$ obtained by CPRM for the glass- and vinylon-fiber filled polymer melts is shown below about 10 s^{-1} in figures 8–10. Figure 8 shows N_1 curves for GF-PE systems. N_1 increases with increasing shear rate and fiber content but approaches to those of PE gradually with increasing shear rate. In the case of VF61-PE systems in figure 9, N_1 increases with shear rate but does not increase monotonically with fiber contents, and increases abnormally at $\Phi_w = 15\%$ of fiber contents. Figure 10 shows the N_1 vs. $\dot{\gamma}$ curves for four kinds of VF filled polyethylene melts with the same fiber content of $\Phi = 7.5\%$. The effect of the aspect ratio on N_1 is clearly shown. In figures 11 and 12, N_1 was plotted against σ_{12} for GF- and VF-PE systems, respectively. The correlation between N_1 and σ_{12} is of great

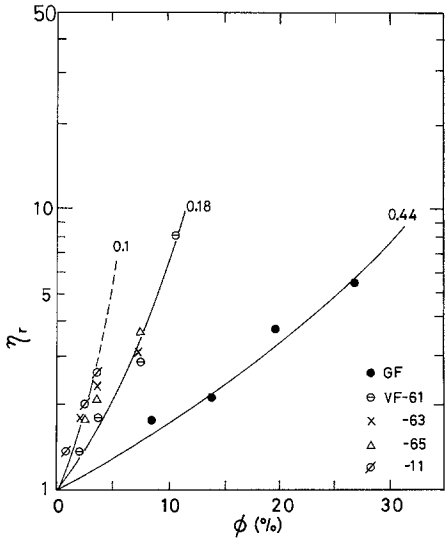

Fig. 7. Relations between relative viscosity η_r and volume fraction of fibers Φ (%) for GF- and VF-PE systems. The numerical values represent the values of A in eq. (10).

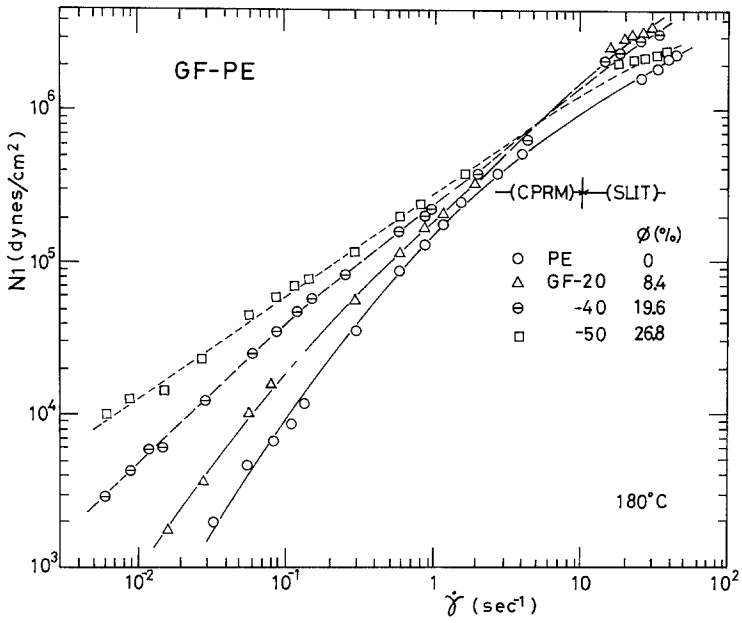

Fig. 8. First normal-stress difference N_1 as a function of shear rate $\dot{\gamma}$ for GF-PE systems at 180 °C.

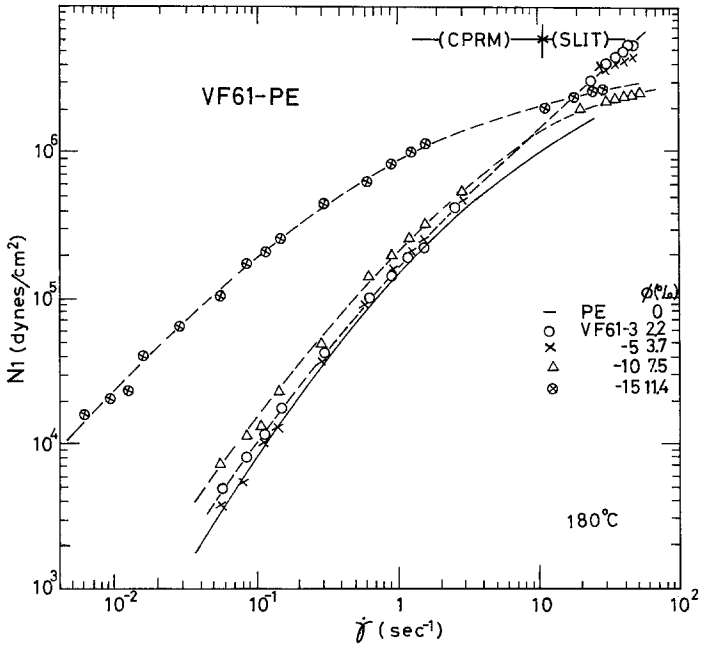

Fig. 9. First normal-stress difference N_1 as a function of shear rate $\dot{\gamma}$ for VF61-PE systems at 180 °C.

interest because it shows the relative influence of the addition of fibers on N_1 and σ_{12} and not the influence of N_1 alone [7].

From the studies of pure melts [17] it is known that N_1 vs. σ_{12} plots are independent of temperature and flexibility of polymer chain backbone but dependent upon molecular weight distribution. It is seen from figure 11 that the increase of N_1 is much greater than σ_{12} for GF-PE systems. The slope of N_1 vs. σ_{12} curves decreases with increasing fiber content. These results are different from those obtained by Czarnecki et al. [7] who reported that the slope of N_1 vs. σ_{12} curves for glass-fiber filled polystyrene melts does not change independent of fiber content. The reason of this difference is not yet understood. The influence of fibers on the $N_1 - \sigma_{12}$ relationship is different from that of small particles [17, 18]. The mechanism which gives large normal stresses in fiber-filled systems is presumably that given by Chan et al. [4–6], who suggested that the shear flow between fibers induces tensile

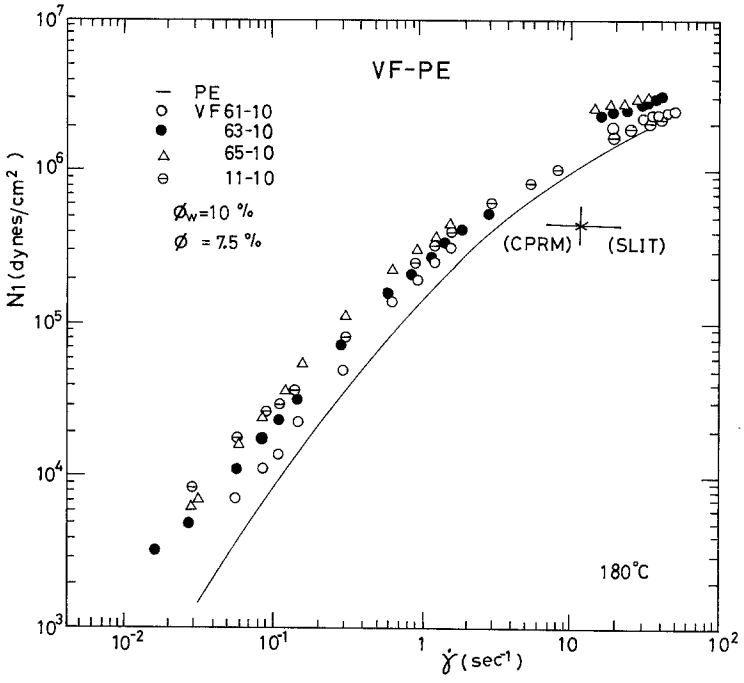

Fig. 10. First normal-stress difference N_1 as a function of shear rate $\dot{\gamma}$ for VE-PE systems with 7.5% volume fraction of vinylon fibers.

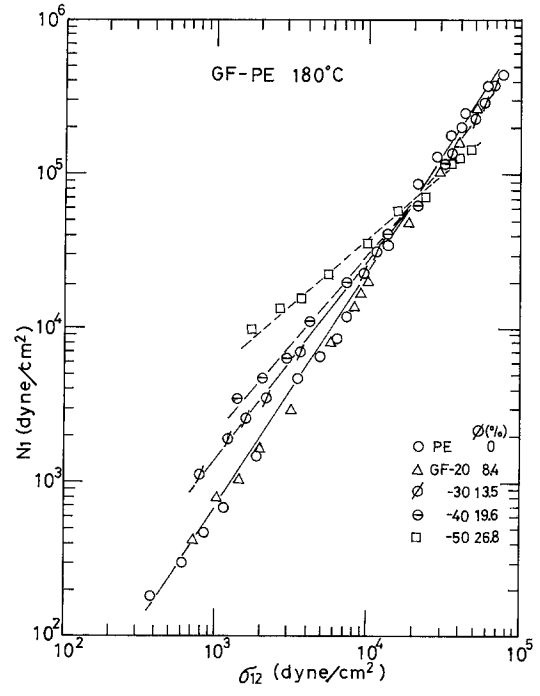

Fig. 11. First normal-stress difference N_1 as a function of shear stress σ_{12} for GF-PE systems.

stresses and the fiber tensile stresses acting along closed streamlines result in a normal stress in the fluid. This phenomenon is due to normal stresses being caused not only by the medium but also by the existence of fibers, as indicated by the Weissenberg rod climbing effects found in suspensions of fibers in Newtonian fluids [19, 20].

Figure 12 shows the relationship between N_1 and σ_{12} for VF-PE systems. These curves are not linear in contrast to those for GF-PE systems (fig. 11). This fact may be attributed to the flexibility of VF.

Czarnecki and White [7] used the following equation to represent the $N_1 - \sigma_{12}$ relationship for the data on homogeneous melts:

$$N_1 = B\sigma_{12}^c. \tag{12}$$

They determined parameters B and c for fiber-filled melts and related B to fiber content and aspect ratio. In these cases, values of the exponent c are independent of fiber content. In our experiments, however, the exponent c for GF-PE systems depends on fiber content. The exponent c for VF-PE systems could not be determined because the data were not linear (fig. 12). It is evident from figure 11 that B is an increasing function of Φ for GF-PE systems.

Figure 13 shows some examples of pressure profiles as a function of L for PE and fiber filled melts in slit flow. The parameter $\dot{\gamma}_w$ in this figure is an apparent wall shear rate according to eq. (4). It is seen from figure 13 that the pressure profiles become linear over the distance along which pressure measurements were taken, indicating that the flow becomes fully developed. From the slope of the pressure profile, the wall shear stress σ_w was determined, and σ_w and η were plotted against $\dot{\gamma}$ (eq. (5)) in figures 2–4.

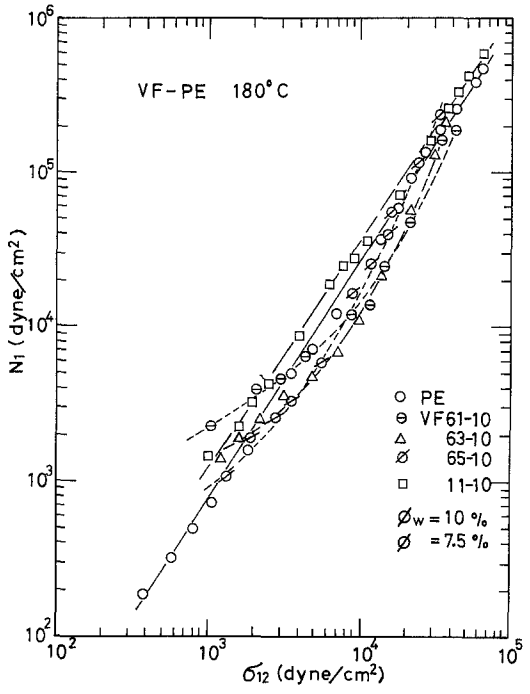

Fig. 12. First normal-stress difference N_1 as a function of shear stress σ_{12} for VF-PE systems with 7.5% volume fraction of vinylon fibers.

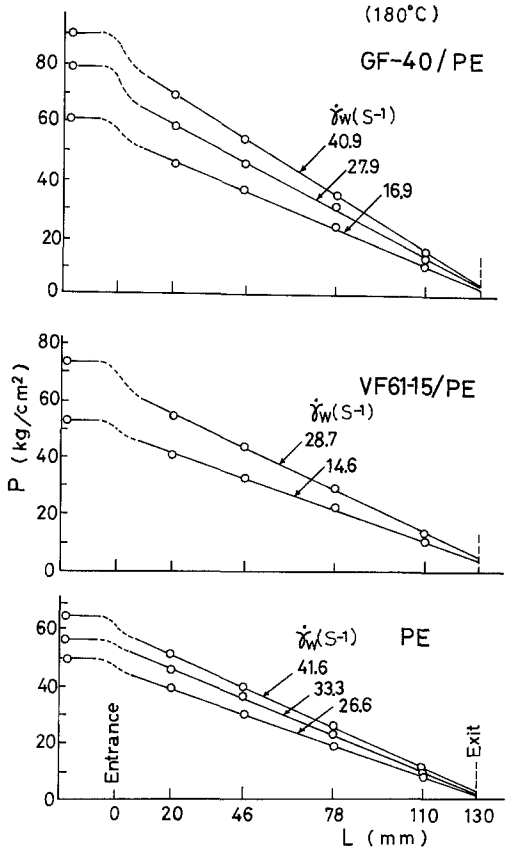

Fig. 13. Pressure profiles of fiber filled polyethylene melts flowing through a slit die.
(a) GF-40/PE, (b) VF61-15/PE, (c) PE.

The exit pressure or the first normal-stress difference as a function of shear rate is plotted in figures 8–10. The data at high shear rates are rather satisfactory, considering the difficulties met in experiments.

In order to examine the flow properties of fiber-filled polymer melts at high shear rates, the capillary flow experiments were carried out by using a capillary viscometer. Plots of wall shear stress σ_w against true shear rate $\dot{\gamma}$ (eq. (8)) for GF- and VF-PE systems are shown in figures 14 and 15, respectively. For GF-PE systems (fig. 14) shear stress increases with increasing shear rate and fiber content even at high shear rates.

A comparison of shear stress curves at high shear rates in figure 2 with those in figure 14 shows that curves for the same systems can not be connected smoothly but data in figure 14 are higher than those in figure 2. For VF61-PE systems (fig. 15), σ_w also increases with increasing $\dot{\gamma}$ and Φ (shown in fig. 15(a)), but the flow curves at low shear rates are connected rather smoothly with those at high shear rates shown

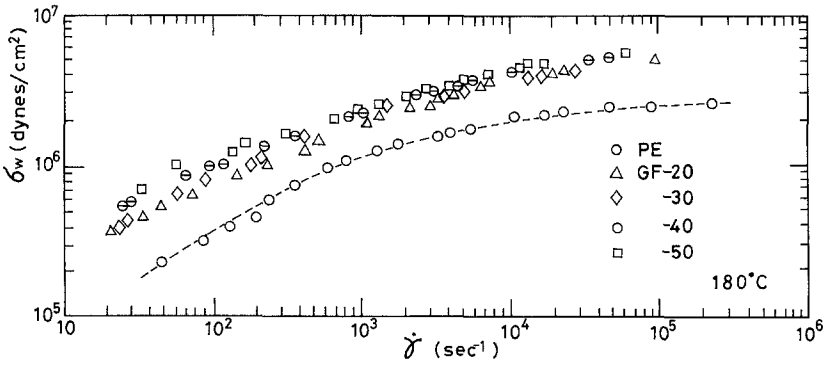

Fig. 14. Flow curves for GF-PE systems at 180 °C.

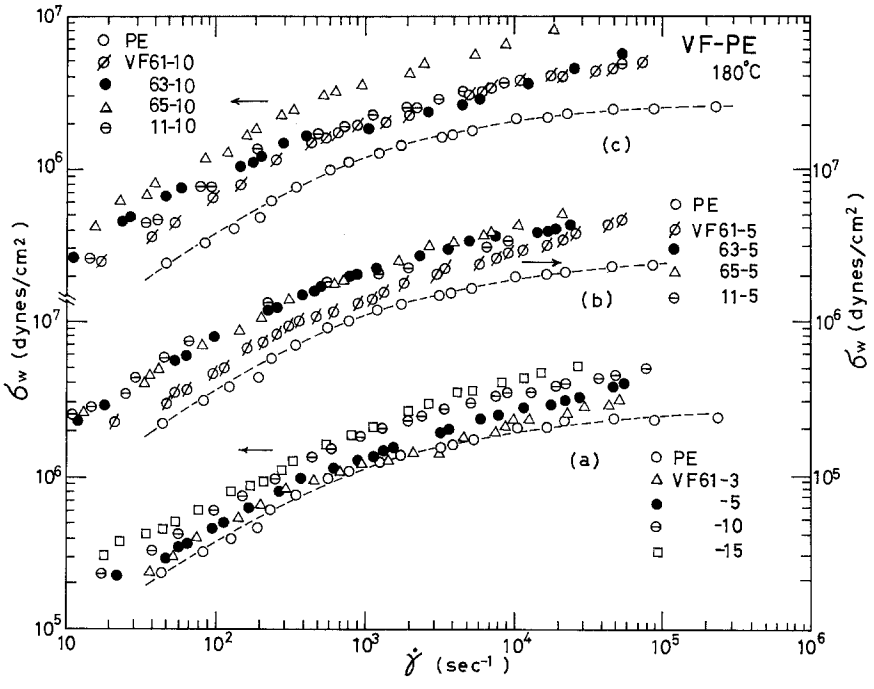

Fig. 15. Flow curves for VF-PE systems at 180 °C.
(a) VF61-PE systems, (b) VF-PE systems with 3.7% of volume fration, (c) VF-PE systems with 7.5% of volume fraction.

in figure 3 although data in figure 15 are slightly higher than those in figure 3.

The higher values obtained by capillary flow may be attributed to the small diameters of the capillaries. Large difference of GF-PE systems in slit and capillary flow data is considered to be due to the rigidity of the fibers. Flow curves in figure 15 (b) and (c) show that σ_w increases slightly with increasing aspect ratio. The flexibility of fibers may also be an important factor for flow properties of fiber-filled systems because of the difference of the structure formed by fibers in polymer melts even in the high shear flow field.

(3) Relative viscosity η_r defined as the ratio of the viscosity of the fiber filled system to that of the medium at the same shear stress increases with increasing a_r and Φ. Likewise the flexibility of fibers affects the relation between η_r and Φ.

(4) By adding fibers N_1 increases more rapidly than σ_{12} at low shear rates but the slope decreases with increasing $\dot{\gamma}$. For GF-PE systems N_1 increases linearly with σ_{12} in log-log plots, but the slope of $N_1 - \sigma_{12}$ curves decreases with increasing Φ. For VF-PE systems $N_1 - \sigma_{12}$ relationship is rather complex.

4. Conclusion

This paper presents the rheological properties of glass- and vinylon-fiber filled polyethylene melts. The influences of aspect ratio a_r, fiber content Φ, flexibility of fibers, shear rate $\dot{\gamma}$ and other factors on the flow properties of the fiber-filled systems were measured over a wide range of shear rate by using three kinds of rheometers. Main results obtained are as follows:

(1) Addition of glass- and vinylon-fibers to polymer melts results in an increase in viscosity or shear stress but does not change the basic character of the viscosity-shear rate relationship of polymer melts over a wide range of shear rates.

(2) Influences of aspect ratio and content on the flow properties of fiber filled systems are remarkable at low shear rates but decrease at high shear rates.

1. Charrier JM, Rieger JM (1974) Fiber Sci Technol 7: 161
2. Oyanagi Y, Yamaguchi Y (1975) J Soc Rheol Japan 3: 64
3. Wu S (1979) Polym Eng Sci 19:638
4. Chan Y, White JL, Oyanagi Y (1978) J Rheol 22: 507
5. Chan Y, White JL, Oyanagi Y (1978) Polym Eng Sci 18:268
6. White JL, Chan Y, Oyanagi Y (1978) J Soc Rheol Japan 6-1:1
7. Czarnecki L, White JL (1980) J Appl Polym Sci 25: 1217
8. Kitano T, Kataoka T (1980) Rheol Acta 19:753
9. Kitano T, Kataoka T, Nishimura T, Sakai T (1980) Rheol Acta 19:764
10. Kitano T, Kataoka T, Shirota T (1981) Rheol Acta 20: 207

11. Walters K (1975) Rheometry. Chapman and Hill, London
12. Han CD, Kim KU (1972) Rheol Acta 11:323
13. Forgacs OL, Mason SG (1959) J Colloid Sci 14:457
14. Kitano T, Kataoka T (1981) Rheol Acta 20:390
15. Kitano T, Kataoka T (1981) Rheol Acta 20:403
16. Oda K, White JL, Clark ES (1978) Polym Eng Sci 18: 25
17. Lobe VM, White JL (1979) Polym Eng Sci 19:617
18. White JL (1979) J Non-Newtonian Fluid Mech 5:177
19. Mewis J, Metzner AB (1974) J Fluid Mech 62:593
20. Maschmeyer RO, Hill CT (1974) Adv Chem Ser 134: 95
21. Data from Kuraray's catalogue

(Received March 2, 1983)

Authors' address:

Dr. T. Kitano, Prof. T. Kataoka, Dr. Y. Nagasuka
Research Institute for Polymers and Textiles
1-1-4 Yatabe-Higashi, Tsukuba
Ibaraki 305 (Japan)